J Neuropathol Exp Neurol
Vol. 67, No. 9
September 2008
pp. 842–856

ORIGINAL ARTICLE

Cerebral Small Vessel Disease-Induced Apolipoprotein E Leakage Is Associated With Alzheimer Disease and the Accumulation of Amyloid β-Protein in Perivascular Astrocytes

Sabrina Utter, Irfan Y. Tamboli, PhD, Jochen Walter, PhD, Ajeet Rijal Upadhaya, MSc, Gerd Birkenmeier, MD, Claus U. Pietrzik, PhD, Estifanos Ghebremedhin, MD, and Dietmar Rudolf Thal, MD

Abstract

Apolipoprotein E (apoE) plays a role in the pathogenesis of Alzheimer disease (AD). It is involved in the receptor-mediated cellular clearance of the amyloid β-protein (Aβ) and in the perivascular drainage of the extracellular fluid. Microvascular changes are also associated with AD and have been discussed as a possible reason for altered perivascular drainage. To further clarify the role of apoE in the perivascular and vascular pathology in AD patients, we studied its occurrence and distribution in the perivascular space, the perivascular neuropil, and in the vessel wall of AD and control cases with and without small vessel disease (SVD). Apolipoprotein E was found in the perivascular space and in the neuropil around arteries of the basal ganglia from control and AD cases disclosing no major differences. Western blot analysis of basal ganglia tissue also revealed no significant differences pertaining to the amount of full-length and C-terminal truncated apoE in AD cases compared with controls. In contrast, Aβ occurred in apoE-positive perivascular astrocytes in AD cases but not in controls. In blood vessels, apoE and immunoglobulin G were detected within the SVD-altered vessel wall. The severity of SVD was associated with the occurrence of apoE in the vessel wall and with that of Aβ in perivascular astrocytes. These results point to an important role of apoE in the perivascular clearance of Aβ in the human brain. The occurrence of apoE and immunoglobulin G in SVD lesions and in the perivascular space suggests that the presence of SVD results in plasma-protein leakage into the brain. It is therefore tempting to speculate that apoE represents a pathogenetic link between SVD and AD.

Key Words: Alzheimer disease, Amyloid β-protein, Apolipoprotein E, Astrocytes, Blood-brain barrier, Small vessel disease.

INTRODUCTION

The deposition of the amyloid β-protein (Aβ) and the formation of neurofibrillary tangles are histopathologic hallmarks of Alzheimer disease (AD) (1–3). Amyloid β-protein deposition can either result from an increased production or aggregation, as seen in familial AD cases, and in transgenic mice or from altered Aβ clearance (4–11). Important clearance mechanisms for Aβ include the cellular clearance by microglial cells and astrocytes (12–17), degradation by proteases such as neprilysin and the insulin-degrading enzyme (6, 18), clearance via the blood-brain barrier (BBB) (9), and drainage along perivascular channels (8).

Apolipoprotein E (apoE) is a plasma lipoprotein constituent that is produced in the liver (19). In the brain, astrocytes and neurons are capable of producing apoE (20, 21). Recently, we have reported that apoE occurs in perivascular drainage channels of wild-type and amyloid precursor protein (APP)–transgenic mice (22). Because the *APOE ε4* allele is a major risk factor for sporadic AD (23), apoE binds Aβ (24, 25), and because the α_2-macroglobulin receptor/low-density lipoprotein receptor-related protein (LRP) is an important receptor for the uptake of apoE-bound Aβ by neurons and astrocytes (26, 27), it has been speculated that binding of apoE to Aβ is critical for Aβ clearance. In fact, LRP is considered to be involved in Aβ clearance through the BBB (9). Perivascular drainage of Aβ has been discussed as a further mechanism for Aβ clearance (8). This is supported by the presence of cerebrovascular Aβ deposits in the human brain and in the brains of transgenic mice producing Aβ almost exclusively in nerve cells (8, 28). The colocalization of Aβ and apoE within the perivascular space of APP-transgenic mice also argues in favor of an apoE-linked perivascular clearance of Aβ (22). In this context, however, it has not been shown whether perivascular spaces in the human brain similarly contain apoE and Aβ and contribute to Aβ clearance.

From the Departments of Neuropathology (SU, DRT) and Neurology, University of Bonn, Bonn (IYT, JW); Institute of Pathology–Laboratory of Neuropathology, University of Ulm, Ulm (ARU, DRT); Department of Biochemistry, University of Leipzig, Leipzig (GB); Institute of Physiological Chemistry and Pathobiochemistry, Molecular Neurodegeneration, University of Mainz, Mainz (CUP); and Institute of Clinical Neuroanatomy, J.W. Goethe University, Frankfurt am Main, (EG), Germany.

Send correspondence and reprint requests to: Dietmar R. Thal, MD, Department of Pathology–Laboratory of Neuropathology, University of Ulm, Albert-Einstein-Allee 11, D-89081 Ulm, Germany; E-mail: Dietmar.Thal@uni-ulm.de

This study was supported by Grant O-154.0041 from the University of Bonn (BONFOR) and by Grant TH624/4-1 from the DFG (D.R.T.).

Human autopsy tissue was studied according to German law for using human tissue in agreement with the votes of the local ethical committees of the Universities of Bonn and Ulm.

Cerebral small vessel disease (SVD) is associated with AD (29–32). Such vascular alterations have been discussed to impact perivascular drainage and BBB function in the brain (8, 33, 34). Although these associations have been reported, a clear pathogenetic link between AD and SVD has not been described so far.

Here, we analyzed the distribution of apoE and Aβ in the perivascular neuropil, the perivascular space, and in intracerebral arteries and veins. Our results provide evidence for the contribution of apoE to both the perivascular clearance of Aβ in the human brain and the development of SVD and suggest a pathogenetic link between SVD and AD.

MATERIALS AND METHODS

Neuropathology

Thirty human autopsy cases (10 AD and 20 non-AD cases; Table) studied extensively for the presence and

TABLE. List of Cases

Number	Age	Sex	CDR	Neuropathologic Diagnosis	Braak Stage	CERAD	Aβ Phase	SVD Stage	CAA Stage	CAA Severity	*APOE* Genotype
a: Cases analyzed histopathologically and immunohistochemically											
1	60	M	0	Control	1	0	0	C	0	0	3/3
2	61	M	0	Control	0	0	0	0	0	0	3/3
3	61	F	0	Infarction; AGD	1	0	0	B	0	0	3/4
4	61	M	0	Cortical micrometastasis of a carcinoma	0	0	0	B	0	0	3/3
5	62	M	0	Control	0	0	0	0	0	0	3/3
6	62	F	0	Control	1	0	0	C	1	1	3/3
7	62	M	0	Control	0	0	0	A	0	0	3/3
8	62	M	0	Control	3	0	4	B	2	2	3/4
9	63	F	0	Multiple cerebral hemorrhagic infarcts	3	1	4	B	0	0	3/3
10	65	M	0	Control	1	0	2	0	0	0	3/4
11	66	F	0	Arteriosclerosis; AGD	0	0	0	C	0	0	3/3
12	66	M	0	Control	1	0	0	B	0	0	2/3
13	68	F	0	Control	2	0	0	A	1	2	3/3
14	69	F	0	Control	0	0	0	0	0	0	2/3
15	73	F	1	Metastasis of a carcinoma left frontal; AGD	1	0	1	A	1	2	2/3
16	77	M	0	Arteriosclerosis; *M. Fahr*	2	0	0	B	0	0	3/3
17	79	F	2	Multiple hemorrhagicinfarcts; AGD	2	0	0	C	0	0	3/3
18	83	F	0	Arteriosclerosis; AGD	3	0	1	C	1	2	3/3
19	84	F	0	Arteriosclerosis; multiple hemorrhagic infarcts; AGD	1	0	1	B	0	0	2/3
20	88	M	2	AGD	2	1	3	B	1	2	2/3
21	78	M	1	AD; CAA	4	1	3	B	1	2	3/3
22	78	F	3	AD; *M. Fahr*	5	2	4	B	2	2	3/4
23	81	F	3	AD; CAA	5	2	4	C	1	2	3/3
24	82	M	2	AD; arteriosclerosis	3	2	3	C	2	2	3/4
25	83	M	3	AD; old infarction; CAA; small pontine hemorrhage	5	2	4	B	3	2	4/4
26	83	M	3	AD; small pseudocystic infarct; plexus choroideus xanthogranuloma	4	2	4	B	2	2	3/3
27	85	M	2	AD; microinfarcts; CAA; mixed dementia	3	2	3	C	3	2	3/4
28	87	F	3	AD; CAA; arteriosclerosis	4	1	4	C	2	2	3/3
29	89	F	3	AD; CAA	5	3	4	C	2	2	3/4
30	89	F	2	AD; CAA; mild arteriosclerosis	4	3	4	B	2	2	3/4
b: Cases used for biochemical analysis											
31	66	M	0	Intracerebral and subarachnoidal hemorrhage	1	0	0	B	0	0	3/3
32	70	M	0	Control	1	0	0	B	0	0	2/3
33	71	F	0	Microinfarction	1	0	0	B	0	0	2/3
34	71	M	0	CAA; SVD	2	0	2	C	1	2	2/4
35	77	F	3	Vascular dementia; pontine hemorrhage	3	1	2	B	0	0	3/3
36	80	F	0	Hypertensive arteriopathy; CAA	2	0	2	C	1	1	3/4
37	62	F	3	AD	6	3	4	B	1	1	3/4
38	64	F	ND	AD; hypertensive arteriopathy	6	3	4	A	1	2	3/4
39	79	F	ND	AD; microinfarction	4	2	3	B	1	2	3/3
40	84	M	3	AD; DLB	6	3	4	B	2	1	3/4
41	91	F	3	AD	4	2	3	C	0	0	ND

Aβ, Amyloid β-protein; AD, Alzheimer disease; AGD, argyrophilic grain dementia; *APOE*, apolipoprotein E; CAA, cerebral amyloid angiopathy; CDR, Clinical Dementia Rating (73); CERAD, Consortium to Establish a Registry for Alzheimer's Disease score (43); DLB, dementia with Lewy bodies; ND, not determined; SVD, small vessel disease.

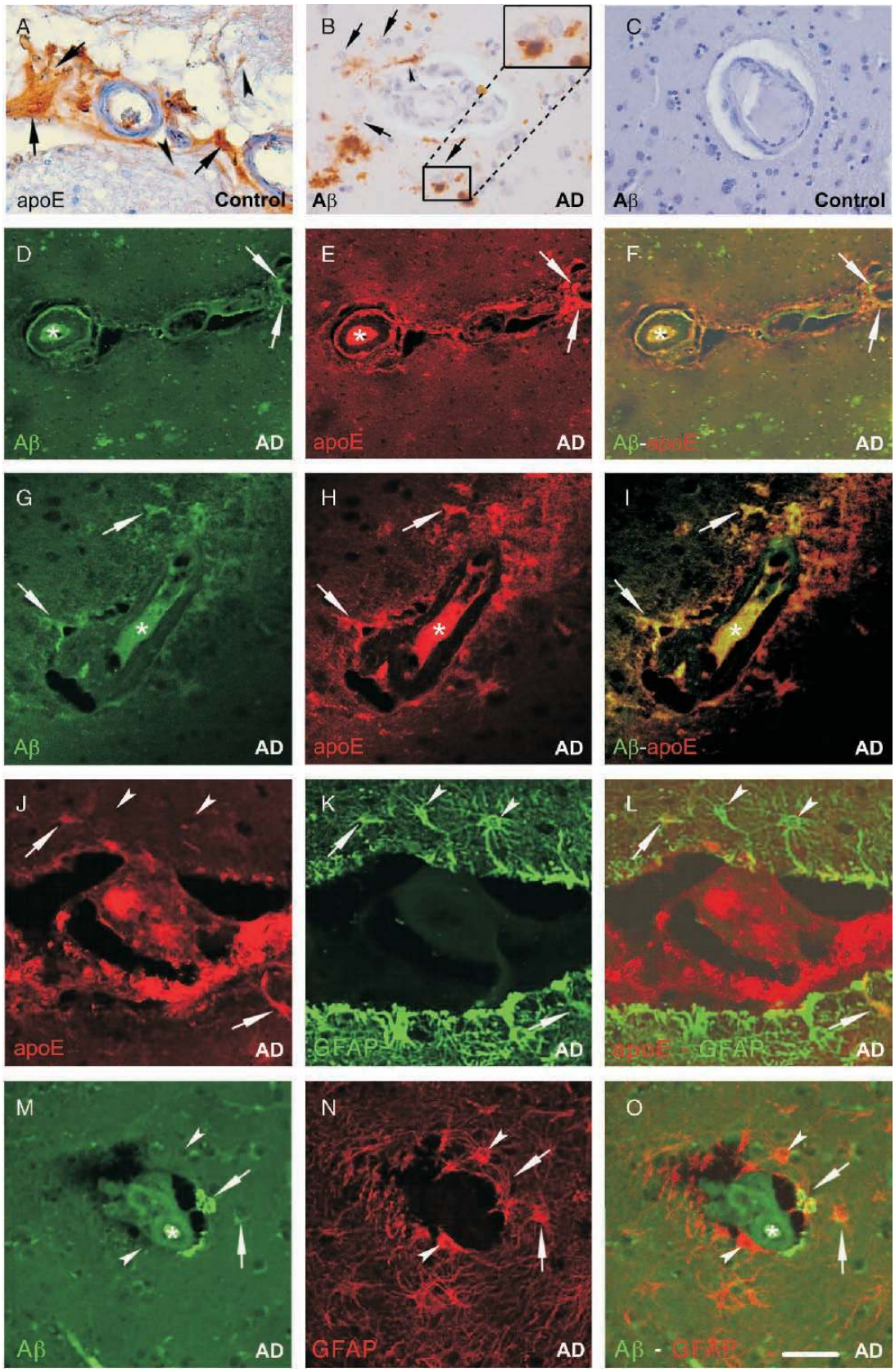

distribution of AD-related changes as published earlier (35) were used to study the distribution of Aβ, apoE, LRP, and immunoglobulin G (IgG) in the basal ganglia.

Demented and nondemented patients had been examined 1 to 4 weeks prior to death according to standardized protocols used for routine clinical and neurologic examination of patients upon admission to the hospital. The protocols included the assessment of cognitive function and recorded the ability to care for and dress oneself, eating habits, bladder and bowel continence, speech patterns, writing and reading skills, short-term and long-term memory, and the orientation within the hospital setting. The Clinical Dementia Rating score (36) was observed retrospectively. These data were used to determine whether individuals clinically fulfilled the *Diagnostic and Statistical Manual of Mental Disorders, Fourth Edition* criteria for dementia (37) or not. Alzheimer disease diagnosis was given in the event that dementia was observed, and AD-related pathology fulfilled recommended criteria for the diagnosis of AD at autopsy (38).

The brains were fixed in a 4% aqueous formaldehyde solution for at least 3 weeks. For the diagnosis of AD-related changes, blocks of the right medial temporal lobe (MTL) were taken at the levels of the 1) anterior limit of the dentate gyrus, 2) lateral geniculate body, and 3) posterior limit of the dentate gyrus (39). The tissue blocks were embedded in polyethylene glycol (Merck-Schuchardt, Hohenbrunn, Germany) (40) and in paraffin. The polyethylene glycol blocks were microtomed at 100 μm, whereas the paraffin sections were cut at 10 μm. Blocks from the basal ganglia, including putamen, globus pallidum, internal and external capsule, claustrum, and the insular cortex, were embedded in paraffin from each case, and 10-μm sections were cut.

Neurofibrillary changes were detected using the Gallyas silver staining method (40, 41). Abnormal phosphorylated tau-protein was recognized with a monoclonal antibody (AT-8; Innogenetics, Ghent, Belgium; 1/1000). The presence of amyloid deposits was assessed using the Campbell-Switzer silver impregnation method (40, 41) and/or using immunohistochemistry with an antibody directed against $A\beta_{17-24}$ (4G8; Covance, Emeryville, CA; 1/5000; formic acid pretreatment). For topographic orientation and neuropathologic diagnosis, serial paraffin and polyethylene glycol sections were stained with aldehyde fuchsin-Darrow-red for lipofuscin pigment and Nissl material. Cytoarchitectural and pigmentoarchitectural parcellation of the entorhinal layers were performed according to Braak and Braak (42). Diagnosis of the stages in the development of neurofibrillary changes (Braak stage) was performed in accordance with published criteria (2, 38). The frequency of neuritic plaques (Consortium to Establish a Registry for Alzheimer's Disease score) was assessed as recommended by Mirra et al (43) on Gallyas-stained sections. For the Braak staging, Consortium to Establish a Registry for Alzheimer's Disease scores, and staging of cerebral amyloid angiopathy (CAA), additional sections from the occipital cortex, including the primary visual cortex, were analyzed. For staging of Aβ pathology, we used the recently described 4 phases of β-amyloidosis in the MTL (44). This hierarchically based procedure enables us to explore the expansion of Aβ-deposition into additional brain regions (44, 45). Phase 1 represents Aβ deposits that are restricted to the temporal neocortex. Phase 2 is characterized by additional Aβ plaques in the entorhinal cortex and/or in the subiculum-CA1 region. The third phase of β-amyloidosis exhibits additional Aβ plaques in the outer zone of the molecular layer of the fascia dentata, subpial band-like amyloid, and/or the presubicular "lake-like" amyloid. The presence of additional Aβ plaques in CA4 and/or the pre-α layer of the entorhinal cortex mark the fourth and final phase of Aβ deposition in the MTL.

The overall expansion of CAA in all autopsy cases was determined according to the 4 stages reported for the development of CAA (30): Stage 0, no CAA; Stage 1, CAA is restricted to neocortical vessels; Stage 2, CAA is seen in neocortical and allocortical vessels and/or in cerebellar vessels; and Stage 3, CAA occurs in the neocortex and allocortex, the cerebellum, the striatum, and in the thalamus. Anti-Aβ-stained or Campbell-Switzer-stained sections of appropriate regions were analyzed.

The severity of CAA was determined in sections of the MTL, occipital cortex, and the basal ganglia. The most severe lesions in these sections were graded according to previously published criteria (46) as follows: 0 (normal), no CAA; 1 (mild), Aβ deposits in the vessel wall without loss of smooth muscle cells in the vessel wall; 2 (moderate), Aβ deposits in the vessel wall accompanied by degeneration of the smooth muscle cell layer; and 3 (severe), extensive Aβ deposition and focal vessel wall fragmentations, microaneurysms, signs of hemorrhage, and fibrinoid necrosis.

Stages for SVD were determined as previously published: SVD Stage 0, no SVD; A, SVD in the basal ganglia; B, SVD also in the thalamus, basal forebrain, cortex, cerebellum,

FIGURE 1. **(A)** Apolipoprotein E (apoE) occurred in the perivascular space (arrows) and in astrocytes of the adjacent neuropil (arrowheads; Case 11). **(B)** In an Alzheimer disease (AD) case (Case 25), perivascular astrocytes contained amyloid β-protein (Aβ)-positive material (arrows), and perivascular Aβ was observed (arrowhead). **(C)** The control case (Case 15) did not exhibit perivascular Aβ or Aβ-positive astrocytes near basal ganglia vessels. **(D–F)** Double label immunofluorescence with antibodies raised against apoE (red) and $A\beta_{17-24}$ (green) showed colocalization of Aβ and apoE within the perivascular space (arrows) of an AD case (Case 25). **(G–I)** Amyloid β-protein-positive perivascular astrocytes (green) in an AD case (Case 25) colocalized apoE (red; arrows). **(J–L)** Double label immunofluorescence with antibodies raised against apoE (red) and glial fibrillary acidic protein (GFAP; green) indicated the astrocytic nature of apoE-positive perivascular cells (arrows). However, a high number of perivascular astrocytes were negative for apoE (arrowheads) in the AD case (Case 25). **(M–O)** Double label immunofluorescence with antibodies raised against $A\beta_{17-24}$ (green) and GFAP (red) confirmed the astrocytic nature of the Aβ-positive perivascular cells in an AD case (Case 25). In **(K)** and **(N)**, the staining for GFAP illustrates that perivascular astrocyte processes contributed to the border between the neuropil and the perivascular (Virchow-Robin) space. *Serum apoE and/or Aβ-positive material in the vessel lumen. Calibration bar on O valid for 80 μm **(A)**; **(B, C, G–O)** 50 μm; **(D–F)** 150 μm.

and the amygdala; C, in addition to the regions affected in Stages A and B, SVD occurs in the brainstem and in the hypothalamus. Hematoxylin and eosin, elastica van Gieson, aldehyde fuchsin-Darrow-red, and anti-Aβ_{17-24}-stained sections were used to categorize the basal ganglia sections neuropathologically.

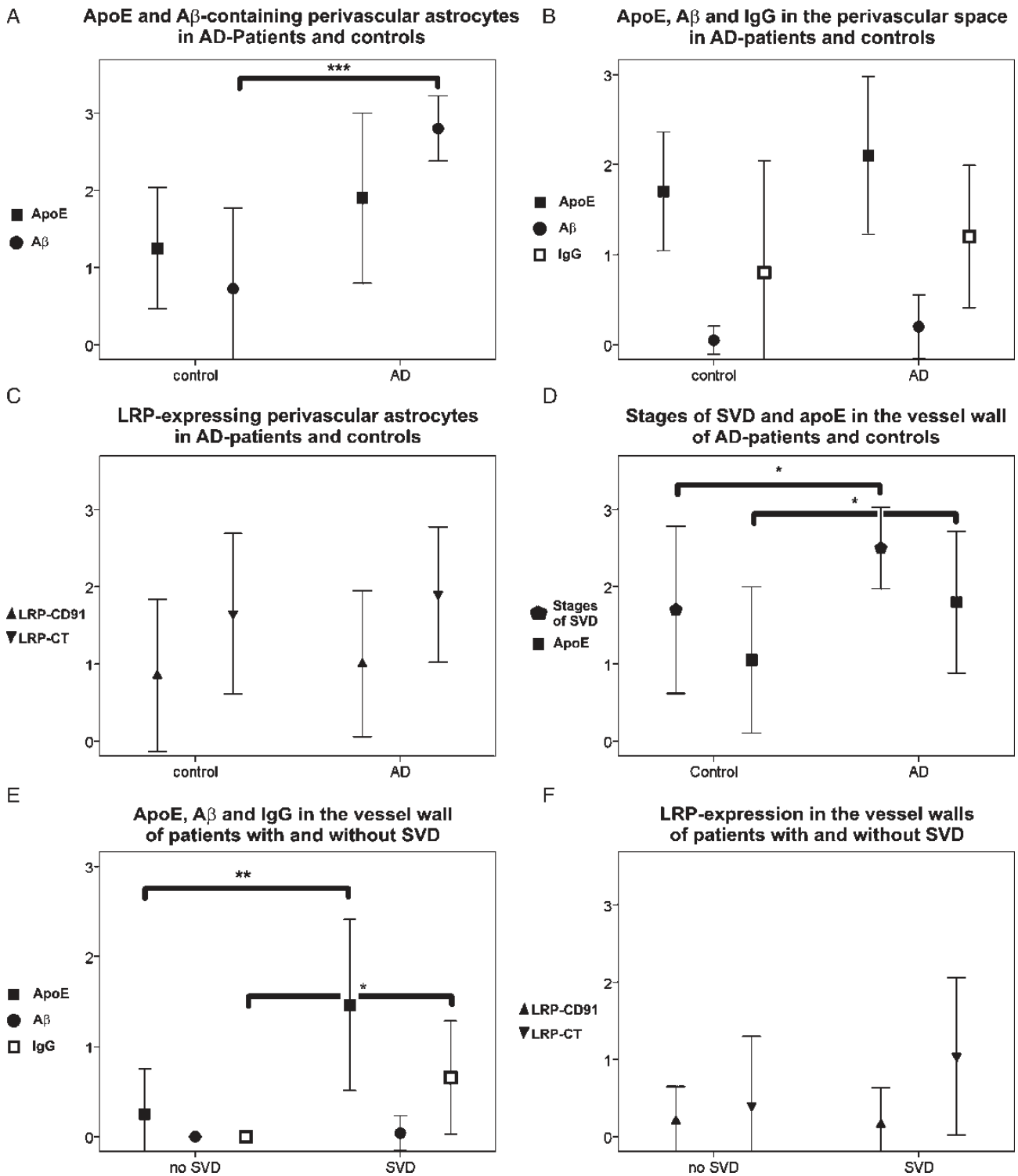

Immunohistochemistry

Paraffin sections (10-μm thick) from the basal ganglia were immunostained with antibodies raised against $A\beta_{17–24}$ (4G8), a synthetic peptide spanning the polymorphic amino acid position 158 of apoE (D6E10; Covance; 1/500; microwave and formic acid pretreatment), the last 15 amino acids of LRP (LRP-1704; polyclonal rabbit antibody [47] 1/50; microwave pretreatment), LRP CD91-α-chain (α2-M-R-II2C7; BioMac, Leipzig, Germany; 1/150; microwave and protease pretreatment), and human IgG (polyclonal goat; Biomeda, Foster City, CA; 1/100; microwave pretreatment). Biotinylated secondary antibodies (avidin-biotin-peroxidase complex kit; Biomeda) were used to detect the primary antibodies and were visualized with the avidin-biotin-peroxidase complex (avidin-biotin-peroxidase complex kit; Biomeda), 3,3-diaminobenzidine-HCl (Sigma-Aldrich, Taufkirchen, Germany), and counterstained with hematoxylin. Positive and negative controls were performed routinely to ensure adequate staining quality.

To verify the presence of Aβ and/or apoE in perivascular astrocytes, smooth muscle cells, and perivascular macrophages and to assess a colocalization of both proteins, double label immunofluorescence has been performed. The term perivascular astrocytes describes astrocytes that are located near the perivascular (Virchow-Robin) space and have processes that contribute to the glial border between the brain and the perivascular space (Figs. 1K, N). Perivascular macrophages are those located within the perivascular space. To test whether Aβ and/or apoE occurs in perivascular astrocytes, we used antibodies directed against the glial fibrillary acidic protein (GFAP; polyclonal rabbit; DAKO, Hamburg, Germany; 1/1000) to detect the astrocytes and anti-$A\beta_{17–24}$ (4G8) or anti-apoE (D6E10). Carbocyanin (Cy)-labeled secondary antibodies (Dianova, Hamburg, Germany) specifically detecting mouse or rabbit IgG were applied in a cocktail. Carbocyanin 2- or Cy3-labeled anti-rabbit IgG and Cy2- or Cy3-labeled anti-mouse IgG were used. For the simultaneous detection of $A\beta_{17-24}$ and apoE, smooth muscle actin (1A4; DAKO; 1/200; microwave pretreatment) and apoE as well as the microglial and macrophage marker CD-68 (PG-M1; DAKO; 1/100; heat pretreatment) and apoE anti-$A\beta_{17–24}$, anti-smooth muscle actin, or anti-CD-68 were applied first and were then visualized with a Cy2- or Cy3-labeled anti-mouse IgG antibody. Subsequently, after absorption of free mouse IgG, the second primary antibody against apoE was applied and visualized with Cy2- or Cy3-labeled anti-mouse IgG. Sections were viewed with a Leica-DMLB fluorescence microscope and a Leica TCS NT confocal laser scanning microscope (Leica, Bensheim, Germany).

Quantitative Western Blot Analysis of apoE in the Basal Ganglia

Fresh tissue from the basal ganglia covering the putamen and the globus pallidus of 1 hemisphere was dissected at autopsy and stored frozen at −80°C until further use. Western blot analysis was performed for 5 AD and 6 control cases (Table; Cases 31–41). The other hemisphere was fixed in a 4% aqueous solution of formaldehyde and processed similarly as described for Cases 1 to 30.

For Western blot analysis, frozen tissue was homogenized in lysis buffer containing 1% Triton X-100 and 1% NP-40. Lysates were centrifuged at 13,200 rpm for 30 minutes at 4°C to obtain supernatants and pellets. Pellets were further resuspended in lysis buffer and homogenized. Supernatants and resuspended pellets were subjected separately to sodium dodecyl sulfate-urea polyacrylamide gel electrophoresis and analyzed by Western immunoblotting with anti-apoE (D6E10) antibody. Actin was detected as loading control.

Using the ImageJ software for densitometric measurements (National Institutes of Health, Bethesda, MD), bands for full-length and C-terminal truncated apoE were measured, and for the pellets, a ratio of C-terminal truncated apoE/full-length apoE was calculated. Cases with a ratio higher than 1 were categorized as C-terminal truncated apoE predominant, and those with a ratio smaller than 1 were categorized as full-length apoE predominant. None of the cases analyzed had a ratio equal to 1.

Semiquantitative Assessment of Perivascular Aβ, apoE, LRP, and IgG

To determine the amount and distribution of apoE and Aβ within the vessel wall, the perivascular space, and in the neighboring neuropil, we semiquantitatively assessed whether and to which degree the perivascular space, neuropil, and the vessel walls were stained with anti-apoE, anti-$A\beta_{17–24}$, and anti-LRP in sections from the basal ganglia. The semiquantitative assessment of LRP expression was performed separately for the α-chain and the C-terminus as detected with the respective antibodies. The following criteria were used for the semiquantitative assessment of the apoE, LRP, IgG, and Aβ expression in the perivascular space, perivascular astrocytes, and within the vessel wall.

For apoE, LRP, IgG, and Aβ expression in the perivascular space, 0 indicates no positive material in the

FIGURE 2. **(A)** Apolipoprotein E (apoE) expression within perivascular astrocytes did not vary significantly in Alzheimer disease (AD) and controls. In contrast, amyloid β-protein (Aβ)-positive perivascular astrocytes more frequently occurred in AD cases than in controls. **(B)** Apolipoprotein E and immunoglobulin G (IgG) occurred within the perivascular space in AD and in non-AD controls without significant differences. Amyloid β-protein-positive material was found in 3 AD and 2 non-AD cases. **(C)** The expression of lipoprotein receptor-related protein (LRP) in perivascular astrocytes detected with the LRP-1704 antibody raised against the LRP-C-terminus (LRP-CT) or the LRP-CD91-α-chain (LRP-CD91) did not vary significantly between AD and non-AD cases. **(D)** The stage of small vessel disease (SVD) in AD patients was higher than in controls. Apolipoprotein E-positive SVD lesions were more frequently found in AD than in non-AD cases. **(E)** Basal ganglia of cases with SVD lesions exhibited apoE- and IgG-positive material in the vessel wall more frequently than in cases free of SVD lesions in the basal ganglia. Except for 1 AD case, there was no Aβ deposition in the basal ganglia vessels. **(F)** There were no significant differences in the expression of LRP in the vessel wall either detectable with antibodies directed against LRP-CT or LRP-CD91. *, $p < 0.05$; **, $p < 0.01$; ***, $p < 0.001$ (Mann-Whitney U test).

perivascular space; 1, the perivascular space contains immunopositive material in up to and including 25% of the vessels of the putamen and the globus pallidus; 2, the perivascular space contains immunopositive material in 26% to 50% of the vessels of the putamen and the globus pallidus; 3, more than 50% of the vessels of the putamen and the globus pallidus contain immunopositive material.

For apoE, LRP, IgG, and Aβ expression in perivascular astrocytes, 0 indicates no immunopositive material in perivascular astrocytes; 1, 1 to 3 astrocytes contain immunopositive

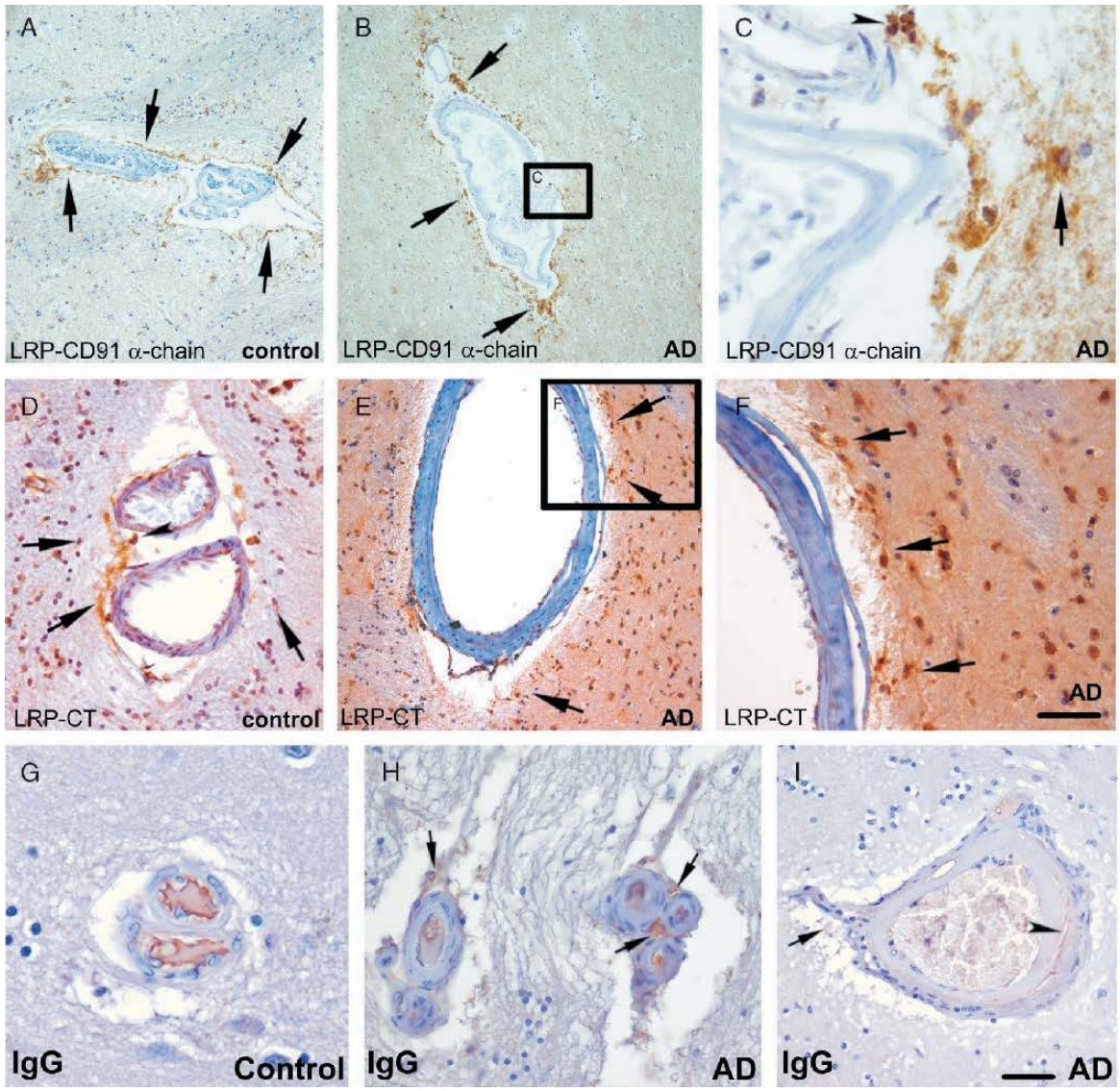

FIGURE 3. **(A–C)** The antibody against LRP-CD91-α-chain perivascular astrocytes (arrow in **C**) and perivascular macrophages (arrowhead in **C**) was stained in the perivascular space of basal ganglia arteries in control **(A)** and Alzheimer disease (AD) cases **(B, C**; Cases 11 **[A]** and 25 **[B, C])**. **(D–F)** A similar staining pattern for LRP was seen with the LRP-1704 antibody raised against the C-terminus of LRP (LRP-CT). Perivascular macrophages (arrowhead in **D**) and astrocytes (arrows in **D**) exhibited LRP-CT in a control **(D)** and an AD case **(E, F**; Cases 4 **[D]** and 26 **[E, F])**. Perivascular astrocytes and perivascular macrophages were labeled with both antibodies. The LRP α-chain was exhibited in the glia limitans around the perivascular space, whereas this border between brain and perivascular space was not highlighted in the staining with anti-LRP-CT except for single cases (data not shown). **(G–I)** Leakage of immunoglobulin G (IgG) into the perivascular space and the vessel wall of cases with small vessel disease (SVD) and AD. **(G)** The basal ganglia artery of a control case without AD and SVD (Case 14) contained IgG-positive plasma only inside the vessel lumen. **(H)** In an AD case with SVD (Case 23), there was extracellular IgG within the perivascular space (arrows). Some perivascular macrophages also contained IgG. **(I)** In another AD case with SVD (Case 28), extracellular IgG was found within the vessel wall (arrowhead). Here, only small amounts of extracellular IgG were detected in the perivascular space (arrow). Calibration bar in **(F)** valid for **(A)** and **(E)** = 150 μm; **(B)** 230 μm; **(C)** 20 μm; **(D)** 75 μm; **(F)** 40 μm. Calibration bar in **(I)** valid for **(G)** = 20 μm; **(H)** 40 μm; **(I)** 50 μm.

material in less than 25% of the vessels in the putamen and the globus pallidus; 2, more than 3 astrocytes contain immunopositive material in less than 50% of the vessels in the putamen and the globus pallidus; 3, more than 3 astrocytes contain immunopositive material in more than 50% of the vessels in the putamen and the globus pallidus.

For apoE, LRP, IgG, and Aβ expression in the vessel wall, 0 indicates no vascular immunopositive material; 1, 1 to

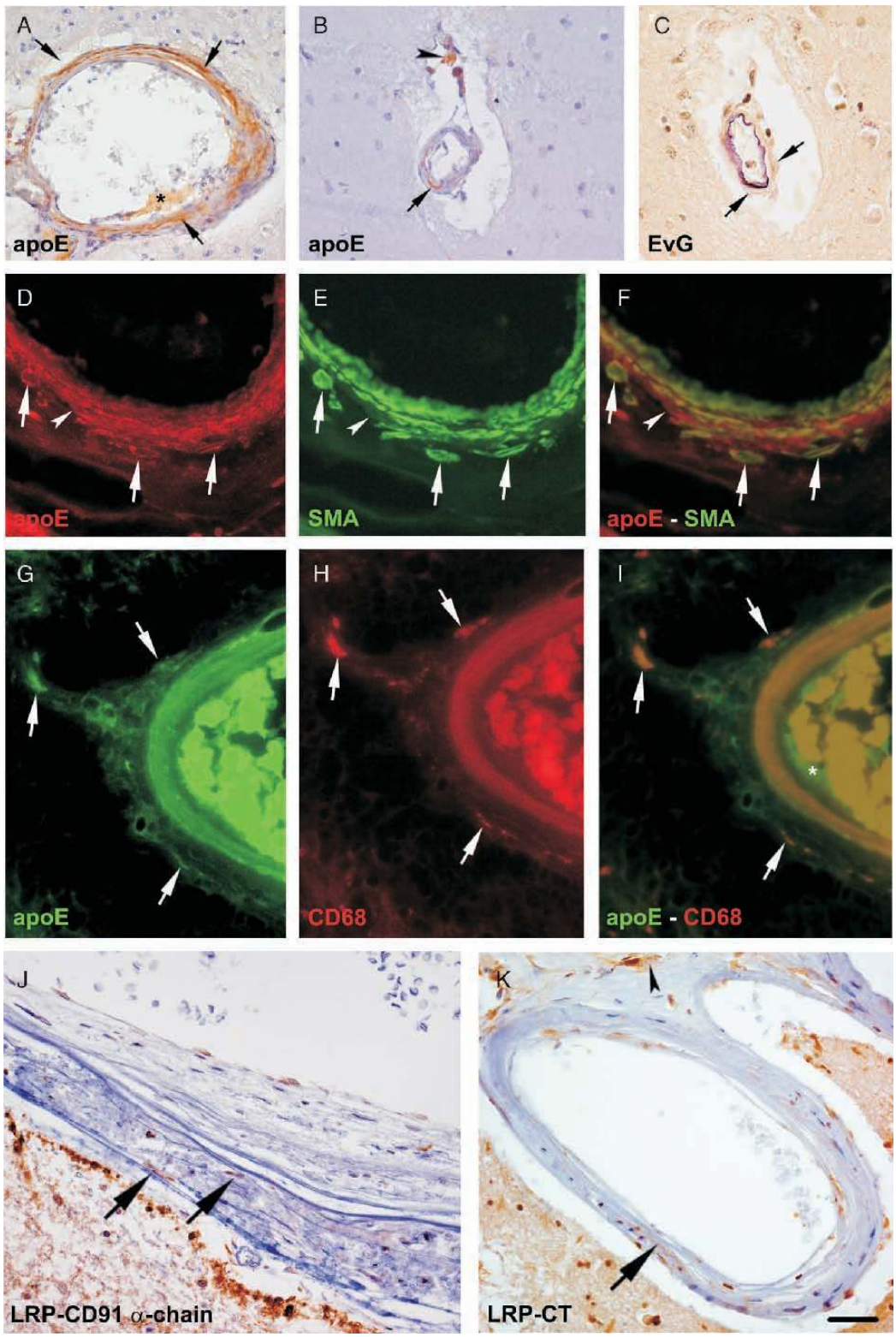

3 vessels with mild affection/expression (<20% of the vessel wall exhibit immunopositive material); 2, 1 to 3 vessels with moderate affection/expression (>20% of the vessel wall exhibit immunopositive material); and 3, more than 3 vessels with moderate to severe affection/expression (>20% of the vessel wall exhibit immunopositive material). Statistical tests were calculated with the SPSS 14.0 program (SPSS, Chicago, IL).

APOE Genotyping

Genomic DNA was extracted either from unfixed frozen brain tissue or from the paraffin-embedded cerebellar cortex. For suitable DNA templates, a 1-step polymerase chain reaction was used, followed by the standard restriction isotyping with the restriction enzyme *Hha*I (48). For DNA templates from formaldehyde-fixed specimens, a seminested polymerase chain reaction assay was used (49). This method facilitates reliable *APOE* genotyping of DNA from archival tissue specimens by enhancing the yield of the polymerase chain reaction product.

RESULTS

Occurrence of apoE and Aβ in the Perivascular Space and in Perivascular Astrocytes

Apolipoprotein E was detected in the perivascular space and in perivascular astrocytes of both AD and control cases (Fig. 1A). Amyloid β-protein was only seen in perivascular astrocytes of AD cases but not in the controls (Figs. 1B, C). Within the perivascular space, Aβ was detected only in 3 AD (Figs. 1D, F) and 2 non-AD cases.

Double label immunofluorescence indicated colocalization of Aβ and apoE within the perivascular space (Figs. 1D–F). Perivascular astrocytes positive for Aβ also exhibited apoE (Figs. 1G–I; arrows). The occurrence of apoE and Aβ in perivascular astrocytes was confirmed by double label immunohistochemistry with anti-GFAP (Figs. 1J–O). However, a high number of GFAP-positive perivascular astrocytes did not exhibit anti-apoE- or anti-Aβ-positive material (Figs. 1M–O). The serum in the blood vessel lumen exhibited apoE and mildly Aβ-positive material (Figs. 1D–I, M–O; asterisks).

Semiquantitative assessment confirmed the general presence of Aβ within perivascular astrocytes in the basal ganglia of AD cases in comparison to that of nondemented controls (Mann-Whitney U test, $p < 0.001$; Fig. 2A). Amyloid β-protein within perivascular astrocytes increased in parallel with the expansion of Aβ plaque deposition as represented by the Aβ phases in the MTL (Kruskal-Wallis H test, $p < 0.001$; trend test, $p < 0.001$) (44), with the expansion of CAA indicated by the CAA stage (Kruskal-Wallis H test, $p < 0.005$; trend test, $p < 0.001$) (30) and with that of neurofibrillary tangles as shown by the Braak stages (Kruskal-Wallis H test, $p < 0.005$; trend test, $p < 0.001$) (2). Apolipoprotein E-positive astrocytes occurred in AD and in control brains (Mann-Whitney U test, $p = 0.12$; Fig. 2A). Significant differences in the apoE expression in perivascular astrocytes among the Aβ phases in the MTL ($p = 0.13$), the CAA stages ($p = 0.51$), and the Braak stages ($p = 0.395$) were not observed. There were no evident differences in the occurrence of apoE and Aβ within the perivascular space of AD cases and nondemented individuals (Mann-Whitney U test: apoE, $p = 0.267$; Aβ, $p = 0.374$; Fig. 2B). Amyloid β-protein-positive material within the perivascular space was thereby found in 3 AD and 2 non-AD cases.

Amyloid β-protein-positive perivascular astrocytes were more frequently found in *APOE ε4* carriers (Mann-Whitney U test; $p < 0.05$), whereas there were no major differences in the occurrence of apoE in the perivascular space (Mann-Whitney U test; $p = 0.505$) and in perivascular astrocytes among the *APOE* genotypes (Mann-Whitney U test; $p = 0.866$).

LRP Expression in Perivascular Astrocytes of AD and Control Cases

Perivascular astrocytes were immunostained with anti-LRP-1704 directed against the C-terminus of LRP and with anti-LRP-CD91 α-chain in similar patterns in AD and control cases (Fig. 3). Likewise, the expression of LRP-positive cells within the perivascular space did not vary significantly between AD and non-AD cases (Fig. 3). The glia limitans was marked with anti-LRP-CD91 α-chain in nearly all cases, whereas anti-LRP-1704 was not prominent in the glia limitans except for single cases.

Semiquantitative assessment of the LRP occurrence in perivascular astrocytes did not exhibit significant differences in our sample between AD and non-AD cases (Fig. 2C) and between *APOE ε4* carriers and noncarriers (Mann-Whitney U test; $p = 0.44$ [LRP-CD91 α-chain]; $p = 0.899$ [LRP-CT]).

Presence of apoE in Vascular Lesions in the Basal Ganglia

Small vessel disease changes were frequently seen especially in arteries of the putamen and the globus pallidus. These changes were observed in 16 controls and

FIGURE 4. **(A)** Apolipoprotein E (apoE)-positive material occurred in the vessel wall of vessels with severe small vessel disease (Case 28). **(B)** In a vessel with only moderate microvascular alterations, apoE-positive material was also found (Case 6). **(C)** The elastica van Gieson-stained adjacent section showed no changes in the vessel wall detectable with this method. **(D–F)** Double label immunofluorescence with antibodies against apoE (red) and smooth muscle actin (SMA; green) identified SMA-positive smooth muscle cells containing apoE (arrows) in Case 30. In addition, between the smooth muscle cells, there was extracellular apoE as well (arrowhead). **(G–H)** Double label immunohistochemistry for apoE (green) and the macrophage marker CD68 (red) demonstrated the macrophage nature of apoE-positive perivascular cells in the adventitia and in the perivascular space (arrows) in Case 28. **(J, K)** LRP was also seen in perivascular macrophages in the vessel wall (arrows) and in the perivascular space (arrowhead in **[K]**). Antibodies against LRP-CD91-α-chain **(J)** and the C-terminus of LRP (LRP-CT; **[K]**) showed similar results in cases 25 **(J)** and 27 **(K)**. *, Serum apoE in the vessel lumen. Calibration bar in **(K)** valid for **(A)** = 60 μm; **(B, C, K)** 40 μm; **(D–F)** 20 μm; **(G–J)** 30 μm.

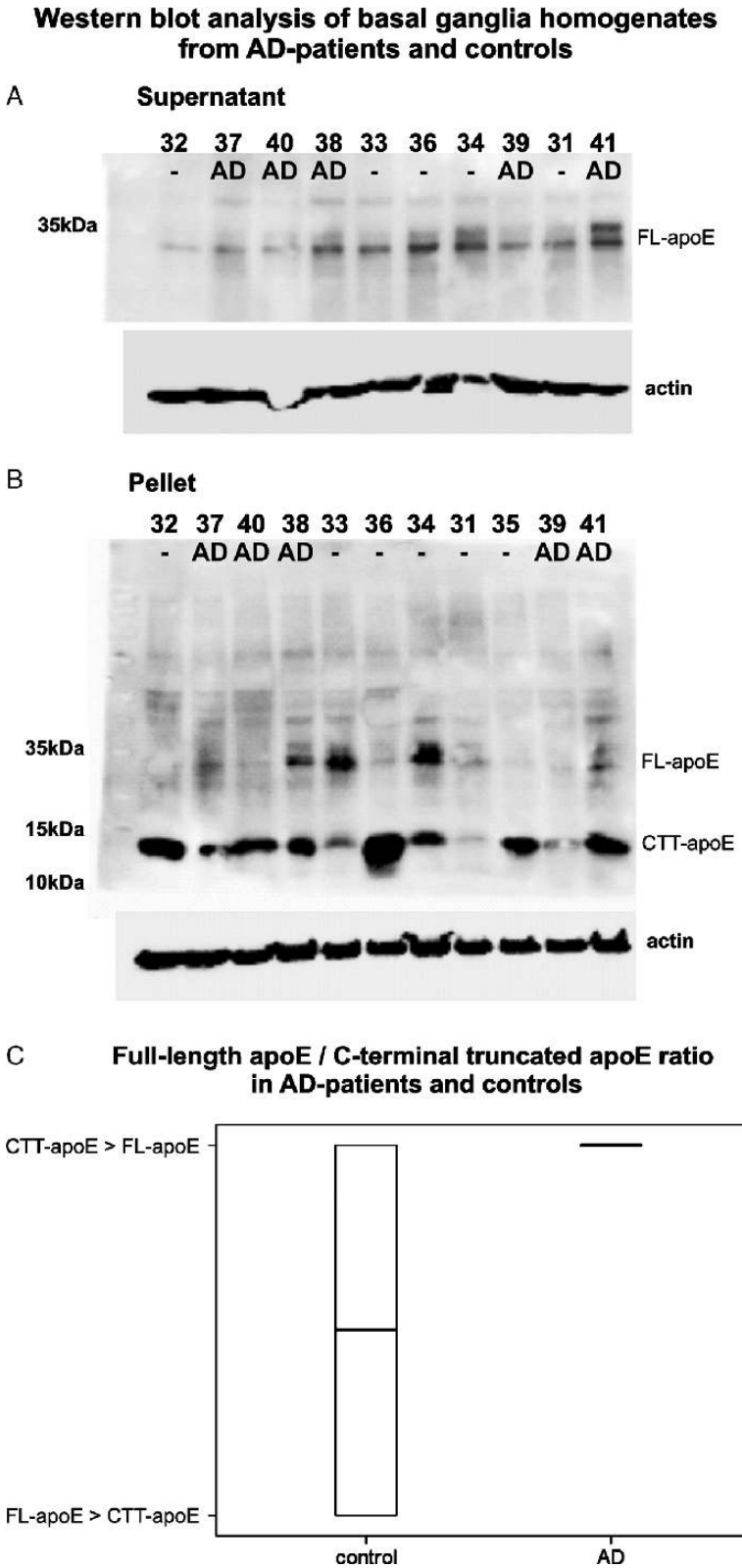

in all 10 AD cases. Four controls were free of SVD. Alzheimer disease cases exhibited SVD more frequently and more widespread as represented by the stage of SVD than controls (Mann-Whitney U test, $p < 0.05$; Fig. 2D). Apolipoprotein E-positive SVD lesions were more frequently found in AD cases than in controls (Mann-Whitney U test, $p < 0.05$; Fig. 2D). Small vessel disease lesions frequently exhibited apoE-expressing cells in the media and extracellular apoE (Figs. 2E, 4A–C; Mann-Whitney U test, $p < 0.005$). There was an overall correlation between the stage of SVD and the exhibition of apoE in the vessel wall (Spearman correlation, $r = 0.331$; $p < 0.05$). Double label immunohistochemistry confirmed the expression of apoE in smooth muscle cells of altered vessels (Figs. 4D–F). Some apoE-positive cells in the vessel wall did not exhibit smooth muscle actin. These cells showed a spindle-shaped morphology and colocalized the CD68 epitope, indicating a macrophage nature of these perivascular cells (Figs. 4G–I). In addition, extracellular apoE was also seen in SVD lesions (Fig. 4F). Apolipoprotein E-positive material in the vessel wall was not only seen in cases with severe SVD but also in those with minimal vascular lesions (Figs. 4B, C). Although cells in the vessel walls were detected with anti-LRP-1704 and anti-LRP-CD91 α-chain (Fig. 4J, K), the occurrence and distribution of these cells did not differ significantly among the stages of SVD and between AD cases and controls ($p = 0.812$; LRP α-chain; LRP-1704; Fig. 2F). Except for 1 AD case with severe CAA, Aβ deposits were not seen in the vessel walls of basal ganglia vessels.

Amyloid β-protein in perivascular astrocytes was more frequently found in cases with advanced SVD stages than in those with early-stage lesions (Kruskal-Wallis H test, $p < 0.05$). Apolipoprotein E in the perivascular astrocytes was not associated with SVD (Kruskal-Wallis H test, $p = 0.476$). Apolipoprotein E ε4 allele carriers did not significantly differ in the vascular apoE and LRP expression from non-ε4 carriers (Mann-Whitney U test; $p = 0.287$–0.687).

IgG in the Perivascular Space of SVD and AD Cases

To clarify whether plasma leakage into the perivascular space and into the vessel wall can explain the occurrence of the plasma protein apoE in the vessel wall and in the perivascular space, the distribution of human IgG was studied in the basal ganglia. All cases (i.e. controls, SVD, and AD cases) exhibited IgG-positive perivascular macrophages. There was no significant exhibition of IgG in perivascular astrocytes. Immunoglobulin G was also detected in the serum inside the blood vessels (Fig. 3G). Small amounts of perivascular IgG were seen only in 1 of 4 control cases free of AD and SVD. In SVD and/or AD cases, on the other hand, extracellular IgG was frequently found in the perivascular space and within the vessel wall of arteries with SVD lesions (Figs. 3H, I).

Semiquantitative assessment of IgG revealed more vessels with IgG-positive lesions in SVD cases when compared with control cases free of SVD (Mann-Whitney U test; $p < 0.05$; Fig. 2E). Significant differences in the amount of IgG in the perivascular space among AD and controls were not seen because 16 of 20 non-AD cases exhibited SVD (Mann-Whitney U test, $p = 0.142$).

Full-Length and C-Terminal Truncated apoE Occur in the Basal Ganglia of AD and Control Cases

Western blot analysis revealed significant amounts of full-length apoE in the supernatant of the basal ganglia tissue lysates. The apoE content varied among all cases without significant differences between AD and control cases (Fig. 5A). The protein pellet of all analyzed cases contained full-length and C-terminal truncated apoE (Fig. 5B). All AD cases thereby showed higher levels of C-terminal truncated apoE than of full-length apoE, whereas predominance of C-terminal truncated apoE was seen in 3 control cases and that of full-length apoE was seen in the other 3 (Figs. 5B, C). The D6E10 anti-apoE antibody is raised against a peptide covering the receptor-binding region of apoE and therefore does not cross-react with C-terminal fragments of apoE but is capable of detecting C-terminal truncated apoE. There were no significant differences in the C-terminal truncated apoE-full-length apoE ratio between *APOE ε4* carriers and noncarriers (Mann-Whitney U test, $p = 0.508$).

DISCUSSION

Our results together with those of our recent studies on animal models (22, 50) show that apoE is not only involved in the perivascular drainage in the pathogenesis of AD but also in that of SVD in the basal ganglia arteries. Therefore, it is tempting to speculate that apoE represents a pathogenetic link between AD and SVD, providing a possible explanation for the previously reported association of AD with SVD (29–32).

Perivascular apoE and its Relation to AD

In this study, we have shown that apoE occurs in the perivascular space and in perivascular astrocytes around the vessels of the basal ganglia of AD and control individuals. Moreover, in AD cases, some of these apoE-positive perivascular astrocytes contained Aβ. The Aβ expression in perivascular astrocytes thereby correlated with the overall expansion of parenchymal and vascular Aβ deposition, as

FIGURE 5. For Western blot analysis, the supernatant of the basal ganglia tissue lysate and the solubilized pellet was subjected. **(A)** The supernatant revealed varying degrees of full-length apolipoprotein E (apoE) in controls (−) and Alzheimer disease (AD) cases. Actin was detected as loading control. **(B)** Within the solubilized pellet, full-length (FL-apoE) and C-terminal truncated apoE (CTT-apoE) were detected. The amounts varied among AD and control samples. The D6E10 anti-apoE antibody detects FL-apoE and apoE-cleavage products containing the receptor-binding domain such as C-terminal truncated apoE, whereas C-terminal fragments cannot be recognized. Actin was detected as loading control. **(C)** All AD cases used for Western blot analysis exhibited more C-terminal truncated apoE than FL-apoE, whereas in controls, this ratio was variable.

represented by the Aβ phases in the MTL (44) and the CAA stages (30), and with that of neurofibrillary changes, as indicated by the Braak stages (2). Combined, our findings in the human brain are in line with previous studies that reported the presence of apoE in perivascular astrocytes and in the perivascular space in the mouse brain (22). The accumulation of Aβ within apoE-positive perivascular astrocytes in AD cases point to a possible involvement of these cells in the pathogenesis of AD. This is supported by 1) the capability of astrocytes to take up Aβ (17); 2) the apoE dependence of this clearance pathway (27); 3) a similar astroglial accumulation of Aβ in association with different types of amyloid plaques (12, 14–16, 51); and 4) the contribution of the latter types of plaques to the development of AD-related β-amyloidosis (44).

The perivascular astrocytes produce apoE and allow drainage of apoE along the perivascular space, as shown in mice overexpressing human apoE driven by an astrocyte-specific GFAP promoter (22). Amyloid β-protein colocalizes apoE in the perivascular space of APP-transgenic mice (22) and of the human brain, as demonstrated here. Thus, Aβ is presumably drained along perivascular channels bound to apoE. Amyloid β-protein deposition in cortical and leptomeningeal vessels is also associated with the deposition of apoE in AD cases (52) and in APP-transgenic mouse models of AD (22) and further argues in favor of this hypothesis.

The accumulation of Aβ in apoE-positive perivascular astrocytes suggests an uptake of apoE-linked Aβ into these cells and to a decreased clearance of these proteins into the perivascular space. The absence of Aβ-positive perivascular astrocytes in APP-transgenic mice (22) indicates that overproduction of Aβ not necessarily leads to the accumulation of Aβ in perivascular astrocytes and argues in favor of clearance deficits that induce the accumulation of Aβ in perivascular astrocytes in sporadic AD cases. The decreased clearance and subsequent accumulation of Aβ may be explained by a BBB dysfunction either at the cellular level or at the vascular level, leading to changes in the composition of the perivascular space fluid.

In detail, astrocytes physiologically clear Aβ across BBB (9). Lipoprotein receptor-related protein is involved in this clearance process (53, 54). The LRP-related clearance of Aβ depends on apoE (26, 27), which is usually produced in the brain by astrocytes (21). In AD, BBB clearance of Aβ is thought to be altered (9, 53). After this hypothesis, one can assume that the function of BBB astrocytes is specifically altered. One would then expect that either changes in the LRP expression or in apoE distribution would accompany Aβ deposition. However, there were no morphologic differences in the perivascular apoE distribution and astroglial LRP expression and no differences in the apoE content of the basal ganglia between AD cases and controls, indicating that glial BBB dysfunction with consecutive changes in the glial LRP expression and the perivascular presence of apoE may not be the key factor for the increase in perivascular Aβ-positive astrocytes. To exclude antibody-specific effects to be responsible for the lack of differences in the cellular LRP expression pattern, we used 2 different antibodies, 1 against the C-terminus of LRP (47) and the other directed against the LRP-CD91 α-chain. The only difference in the staining pattern was a distinct staining of the glia limitans membrane with anti-LRP-CD91 α-chain but not with anti-LRP-1704 directed against the C-terminus. Differences between AD, SVD, and control cases in the LRP staining pattern of the glia limitans were not obvious. Because LRP shedding by metalloproteases has been reported (55), the LRP α-chain-positive material may represent N-terminal shedding products of LRP found in the glia limitans.

A specific accumulation of Aβ in perivascular astrocytes due to glial BBB alterations is also not likely because morphologically similar Aβ-containing astrocytes have also been reported elsewhere, that is, in association with different types of amyloid plaques and within the subpial zone of the molecular layer (12, 14–16, 51). In so doing, perivascular Aβ-containing astrocytes may be a secondary result of altered perivascular drainage, rather than a key event for the reduction of cellular Aβ clearance.

The occurrence of predominantly C-terminal truncated apoE in AD cases (56) indicates significant proteolysis of neuron-derived apoE in AD cases (20). In the event of sufficient apoE drainage, an accumulation of C-terminal truncated apoE would not be expected. Its predominant accumulation in AD cases therefore argues in favor of alterations of the clearance of apoE in addition to that of Aβ. As seen in this study, the presence of C-terminal truncated apoE in control cases with minor AD-related pathology points to an early involvement of clearance alterations for apoE in the pathogenesis of AD at least in the basal ganglia.

Previous studies did not find C-terminal truncated apoE in control cortex (56). Because these studies included only single *APOE ε3/3* control cases (56) and were based on cortex tissue, our finding of predominant C-terminal truncated apoE in the basal ganglia in a subset of control cases, also including *APOE ε2* and *ε4* carriers, does not necessarily contradict these previous reports. The low level of C-terminal truncated apoE in other controls argues in favor of either "normal" variations in the occurrence of C-terminal truncated apoE or initial changes in the equilibrium between full-length and C-terminal truncated apoE. However, the presence of apoE in the brain supports Aβ deposition (57) and is injurious in supporting the accumulation of Aβ in the ubiquitin/proteasome system (58). In doing so, the increased degradation of apoE, as seen here in all AD cases, may indicate that apoE occupies the ubiquitin/proteasome system and thereby induces the intracellular accumulation of Aβ (58).

apoE in SVD

Our second finding was the presence of apoE in the vessel wall of basal ganglia arteries with SVD. Here, apoE was seen in altered smooth muscle cells and in the extracellular space of the lamina media. In single cases, the occurrence of apoE seemed to be a very early sign of SVD. Healthy vessels did not exhibit apoE, as documented here and already reported by others (59). The extent of vessels with apoE-positive cells and/or extracellular apoE in the basal ganglia correlated with the increasing severity of SVD. Regardless of the particular role of apoE, its simple presence in SVD-affected vessels and

its correlation with the stage of SVD indicate that apoE is involved in the pathogenesis of SVD. This is supported by the association of SVD with the *APOE ε4* allele, as found by other authors (60), and the role of apoE in the inhibition of smooth muscle cell proliferation and migration (61, 62). To clarify whether apoE in the vessel wall is produced by local cells or represents plasma leakage into the altered vessel wall, we analyzed whether IgG (a second plasma protein, which is neither produced by smooth muscle cells nor by brain cells) also occurred in the SVD-related vessel wall lesions and in the perivascular space. The detection of IgG within SVD lesions in the vessel wall and its occurrence in the perivascular spaces of SVD and AD patients but not in non-SVD controls strongly suggests a leakage of plasma proteins, including apoE and IgG, into the vessel wall and the perivascular space in SVD and AD patients. This hypothesis is supported by the detection of other serum proteins, including the lipoprotein apoB in association with parenchymal and/or vascular Aβ deposits and in association with cortical vessels in vascular dementia (63–68). Moreover, SVD leads to alterations of the vessel wall similar to hypertensive arteriopathy, and it is obvious that plasma proteins similarly enter the altered vessel wall as reported for hypertensive arteriopathy (33, 34). Further evidence that such vascular lesions support AD-related Aβ deposition has been recently provided by the detection of Aβ deposits in mouse models of hypertension (69).

The presence and extent of SVD are increased in AD cases compared with nondemented controls (29, 30) and suggests a pathogenetic link between AD and SVD. The association of both AD and SVD with the *ε4* allele (23, 60) and the presence of apoE in senile plaques (52) and in SVD-affected vessels, as shown here, provide evidence that this link may be apoE. If this hypothesis is true, the question arises whether AD causes SVD or vice versa, or whether apoE triggers both diseases independently.

Studies in aged APP-transgenic and wild-type mice revealed no SVD-related changes, indicating that SVD is not induced by AD-related plaque deposition and Aβ drainage along perivascular spaces (50). Apolipoprotein E knockout mice reveal vascular changes and are a well-known animal model for atherosclerosis (70). The presence of apoE is assumed to be protective for the vessel wall (59) and also prevents BBB dysfunction (71, 72). It is therefore unlikely that apoE triggers SVD, but the occurrence of apoE may either indicate the upregulation of a feedback mechanism for the inhibition of smooth muscle cell and endothelial cell proliferation and migration (59, 61, 62) or plasma protein leakage. Our finding of an IgG leakage into the vessel wall and into the perivascular space of SVD and AD cases and

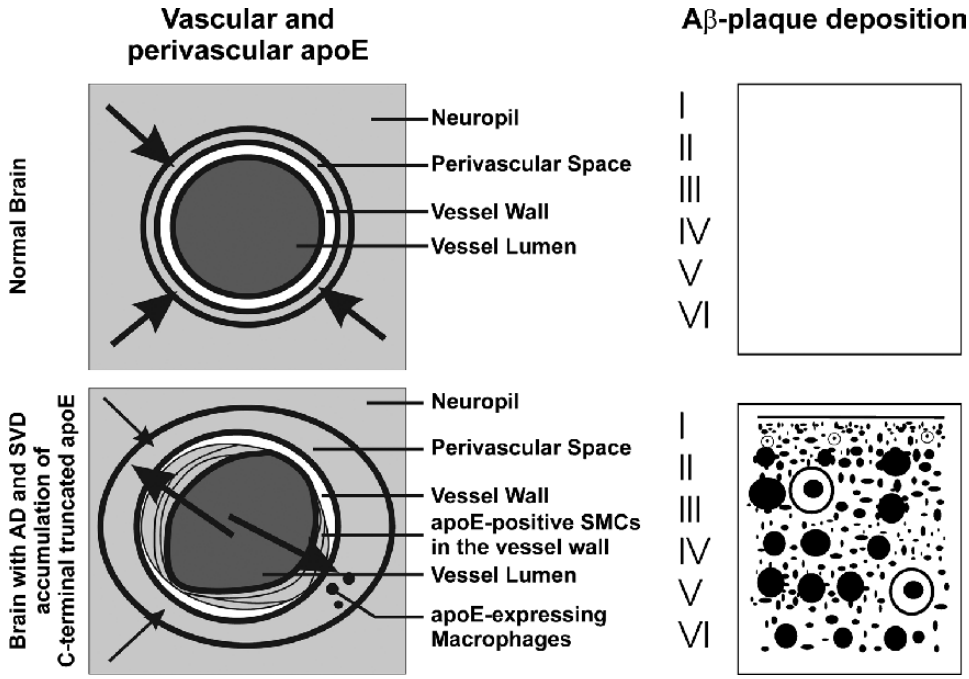

FIGURE 6. Schematic representation of small vessel disease (SVD)–induced plasma protein leakage and its hypothetical consequences. In the normal brain, there is significant efflux of cerebral apolipoprotein E (apoE) into the perivascular drainage channels, as also shown in transgenic mice producing apoE driven by the glia-specific glial fibrillary acidic protein promoter (upper panel) (22). Physiologically produced amyloid β-protein (Aβ) is cleared together with apoE into these channels, and Aβ deposits do not develop. Small vessel disease lesions allow leakage of plasma-proteins into the vessel wall and into the perivascular space (lower panel) (34, 64). Although the glia limitans is still intact, apoE and immunoglobulin G occur in the vessel wall and in the perivascular space of cerebral arteries may therefore compete with brain-derived clearance of apoE from perivascular astrocytes into the perivascular drainage channels. In doing so, one would expect that less Aβ and apoE can be cleared by perivascular drainage. Apolipoprotein E may undergo proteolytic cleavage, and C-terminal truncated apoE predominates in the brain as shown here. The accumulation of Aβ in the brain finally results in the deposition of Aβ and in the development of Alzheimer disease (AD). This hypothesis is supported by the association of the overall expansion of SVD with the development of AD (29, 30).

previously published studies on the presence of plasma proteins, including the lipoprotein apoB, in the AD and vascular dementia brain (63–68) support the latter explanation. Because drainage of cerebral apoE and apoE-linked Aβ into the perivascular space is one of its physiologic clearance mechanisms (22), it is tempting to speculate that leakage of plasma proteins, including apoE, into the perivascular space due to SVD-induced plasma protein leakage raises the threshold for the apoE clearance from the brain. One would expect that the apoE-linked astroglial clearance of Aβ from brain is reduced and thereby leads to the accumulation of Aβ in perivascular astrocytes (Fig. 6) and to the proteolysis of cerebral apoE as indicated by the predominant occurrence of C-terminal truncated apoE in AD cases. Thus, it is tempting to speculate that the competition for perivascular apoE drainage may reduce the cerebral apoE and apoE-linked Aβ clearance in the event that additional apoE due to SVD-related plasma protein leakage needs to be drained and disables the perivascular drainage equilibrium (Fig. 6).

CONCLUSIONS

In the context of recent studies in mouse models (22, 50), our results indicate that 1) apoE plays an important role in the perivascular drainage of the human brain, 2) apoE is involved in the pathogenesis of SVD, and 3) apoE may provide a link between SVD and AD.

ACKNOWLEDGMENTS

The authors thank I. Lungrin, K. Pruy, and H. U. Klatt for technical assistance.

REFERENCES

1. Alzheimer A. Ueber eine eigenartige Erkrankung der Hirnrinde. Allg Zschr Psych 1907;64:146–48
2. Braak H, Braak E. Neuropathological staging of Alzheimer-related changes. Acta Neuropathol 1991;82:239–59
3. Masters CL, Simms G, Weinman NA, et al. Amyloid plaque core protein in Alzheimer disease and Down syndrome. Proc Natl Acad Sci U S A 1985;82:4245–49
4. Games D, Adams D, Alessandrini R, et al. Alzheimer-type neuropathology in transgenic mice overexpressing V717F beta-amyloid precursor protein. Nature 1995;373:523–27
5. Hsiao K, Chapman P, Nilsen S, et al. Correlative memory deficits, Abeta elevation, and amyloid plaques in transgenic mice. Science 1996;274: 99–102
6. Iwata N, Tsubuki S, Takaki Y, et al. Identification of the major Abeta1-42–degrading catabolic pathway in brain parenchyma: Suppression leads to biochemical and pathological deposition. Nat Med 2000;6: 143–50
7. Sturchler-Pierrat C, Abramowski D, Duke M, et al. Two amyloid precursor protein transgenic mouse models with Alzheimer disease–like pathology. Proc Natl Acad Sci U S A 1997;94:13287–92
8. Weller RO, Massey A, Newman TA, et al. Cerebral amyloid angiopathy: Amyloid beta accumulates in putative interstitial fluid drainage pathways in Alzheimer's disease. Am J Pathol 1998;153:725–33
9. Zlokovic BV. Neurovascular mechanisms of Alzheimer's neurodegeneration. Trends Neurosci 2005;28:202–8
10. Mann DM, Iwatsubo T, Cairns NJ, et al. Amyloid beta protein (Abeta) deposition in chromosome 14-linked Alzheimer's disease: Predominance of Abeta42(43). Ann Neurol 1996;40:149–56
11. Mehta ND, Refolo LM, Eckman C, et al. Increased Abeta42(43) from cell lines expressing presenilin 1 mutations. Ann Neurol 1998;43: 256–58
12. Akiyama H, Schwab C, Kondo H, et al. Granules in glial cells of patients with Alzheimer's disease are immunopositive for C-terminal sequences of beta-amyloid protein. Neurosci Lett 1996;206:169–72
13. Schenk D, Barbour R, Dunn W, et al. Immunization with amyloid-beta attenuates Alzheimer-disease–like pathology in the PDAPP mouse. Nature 1999;400:173–77
14. Funato H, Yoshimura M, Yamazaki T, et al. Astrocytes containing amyloid beta-protein (Abeta)–positive granules are associated with Abeta40-positive diffuse plaques in the aged human brain. Am J Pathol 1998;152:983–92
15. Thal DR, Hartig W, Schober R. Diffuse plaques in the molecular layer show intracellular A beta(8–17)–immunoreactive deposits in subpial astrocytes. Clin Neuropathol 1999;18:226–31
16. Yamaguchi H, Sugihara S, Ogawa A, et al. Diffuse plaques associated with astroglial amyloid beta protein, possibly showing a disappearing stage of senile plaques. Acta Neuropathol (Berl) 1998;95:217–22
17. Wyss-Coray T, Loike JD, Brionne TC, et al. Adult mouse astrocytes degrade amyloid-beta in vitro and in situ. Nat Med 2003;9:453–57
18. Leissring MA, Farris W, Chang AY, et al. Enhanced proteolysis of beta-amyloid in APP transgenic mice prevents plaque formation, secondary pathology, and premature death. Neuron 2003;40:1087–93
19. Mahley RW. Apolipoprotein E: Cholesterol transport protein with expanding role in cell biology. Science 1988;240:622–30
20. Brecht WJ, Harris FM, Chang S, et al. Neuron-specific apolipoprotein e4 proteolysis is associated with increased tau phosphorylation in brains of transgenic mice. J Neurosci 2004;24:2527–34
21. Pitas RE, Boyles JK, Lee SH, et al. Astrocytes synthesize apolipoprotein E and metabolize apolipoprotein E–containing lipoproteins. Biochim Biophys Acta 1987;917:148–61
22. Thal DR, Larionov S, Abramowski D, et al. Occurrence and co-localization of amyloid beta-protein and apolipoprotein E in perivascular drainage channels of wild-type and APP-transgenic mice. Neurobiol Aging 2007;28:1221–30
23. Corder EH, Saunders AM, Strittmatter WJ, et al. Gene dose of apolipoprotein E type 4 allele and the risk of Alzheimer's disease in late onset families. Science 1993;261:921–23
24. Sadowski M, Pankiewicz J, Scholtzova H, et al. A synthetic peptide blocking the apolipoprotein E/beta-amyloid binding mitigates beta-amyloid toxicity and fibril formation in vitro and reduces beta-amyloid plaques in transgenic mice. Am J Pathol 2004;165:937–48
25. Strittmatter WJ, Saunders AM, Schmechel D, et al. Apolipoprotein E: High-avidity binding to beta-amyloid and increased frequency of type 4 allele in late-onset familial Alzheimer disease. Proc Natl Acad Sci U S A 1993;90:1977–81
26. Rebeck GW, Reiter JS, Strickland DK, Hyman BT. Apolipoprotein E in sporadic Alzheimer's disease: Allelic variation and receptor interactions. Neuron 1993;11:575–80
27. Koistinaho M, Lin S, Wu X, et al. Apolipoprotein E promotes astrocyte colocalization and degradation of deposited amyloid-beta peptides. Nat Med 2004;10:719–26
28. Calhoun ME, Burgermeister P, Phinney AL, et al. Neuronal overexpression of mutant amyloid precursor protein results in prominent deposition of cerebrovascular amyloid. Proc Natl Acad Sci U S A 1999; 96:14088–93
29. Brun A, Englund E. A white matter disorder in dementia of the Alzheimer type: A pathoanatomical study. Ann Neurol 1986;19:253–62
30. Thal DR, Ghebremedhin E, Orantes M, Wiestler OD. Vascular pathology in Alzheimer's disease: Correlation of cerebral amyloid angiopathy and arteriosclerosis/lipohyalinosis with cognitive decline. J Neuropathol Exp Neurol 2003;62:1287–301
31. Kalaria RN, Ballard C. Overlap between pathology of Alzheimer disease and vascular dementia. Alzheimer Dis Assoc Disord 1999;13:S115–23
32. Skoog I, Kalaria RN, Breteler MM. Vascular factors and Alzheimer disease. Alzheimer Dis Assoc Disord 1999;13:S106–14
33. Scholler K, Trinkl A, Klopotowski M, et al. Characterization of microvascular basal lamina damage and blood-brain barrier dysfunction following subarachnoid hemorrhage in rats. Brain Res 2007;1142: 237–46
34. Nag S, Robertson DM. The brain in hypertension. In: Kalimo H, ed. *Pathology & Genetics: Cerebrovascular Diseases*. Basel, Switzerland: ISN Neuropath Press, 2005;286–92
35. Thal DR, Schultz C, Botez G, et al. The impact of argyrophilic grain

disease on the development of dementia and its relationship to concurrent Alzheimer's disease–related pathology. Neuropathol Appl Neurobiol 2005;31:270–79
36. Hughes CP, Berg L, Danziger WL, et al. A new clinical scale for the staging of dementia. Br J Psychiatry 1982;140:566–72
37. American Psychiatric Association. *Diagnostic and Statistical Manual of Mental Disorders*. 4th ed. Washington DC: American Psychiatric Association, 1994
38. The National Institute on Aging, and Reagan Institute Working Group. Consensus recommendations for the postmortem diagnosis of Alzheimer's disease. The National Institute on Aging, and Reagan Institute Working Group on diagnostic criteria for the neuropathological assessment of Alzheimer's disease. Neurobiol Aging 1997;18:S1–2
39. Insausti R, Amaral DG. Hippocampal formation. In: Paxinos G, Mai JK, eds. *The Human Nervous System*. 2nd ed. London, England: Elsevier, 2004:872–914
40. Braak H, Braak E. Demonstration of amyloid deposits and neurofibrillary changes in whole brain sections. Brain Pathol 1991;1:213–16
41. Iqbal K, Braak H, Braak E, Grundke-Iqbal I. Silver labeling of Alzheimer neurofibrillary changes and brain beta-amyloid. J Histotechnol 1993;16: 335–42
42. Braak H, Braak E. The human entorhinal cortex: Normal morphology and lamina-specific pathology in various diseases. Neurosci Res 1992; 15:6–31
43. Mirra SS, Heyman A, McKeel D, et al. The Consortium to Establish a Registry for Alzheimer's Disease (CERAD). Part II. Standardization of the neuropathologic assessment of Alzheimer's disease. Neurology 1991;41:479–86
44. Thal DR, Rüb U, Schultz C, et al. Sequence of Abeta-protein deposition in the human medial temporal lobe. J Neuropathol Exp Neurol 2000;59: 733–48
45. Thal DR, Rüb U, Orantes M, Braak H. Phases of Abeta-deposition in the human brain and its relevance for the development of AD. Neurology 2002;58:1791–800
46. Vonsattel JP, Myers RH, Hedley-Whyte ET, et al. Cerebral amyloid angiopathy without and with cerebral hemorrhages: A comparative histological study. Ann Neurol 1991;30:637–49
47. Pietrzik CU, Busse T, Merriam DE, et al. The cytoplasmic domain of the LDL receptor–related protein regulates multiple steps in APP processing. EMBO J 2002;21:5691–700
48. Wenham PR, Price WH, Blandell G. Apolipoprotein E genotyping by one-stage PCR. Lancet 1991;337:1158–59
49. Ghebremedhin E, Braak H, Braak E, Sahm J. Improved method facilitates reliable APOE genotyping of genomic DNA extracted from formaldehyde-fixed pathology specimens. J Neurosci Methods 1998;79:229–31
50. Thal DR, Capetillo-Zarate E, Larionov S, et al. Capillary cerebral amyloid angiopathy is associated with vessel occlusion and cerebral blood flow disturbances. Neurobiol Aging. 2008 [Epub ahead of print]
51. Thal DR, Schultz C, Dehghani F, et al. Amyloid beta-protein (Abeta)–containing astrocytes are located preferentially near N-terminal–truncated Abeta deposits in the human entorhinal cortex. Acta Neuropathol (Berl) 2000;100:608–17
52. Namba Y, Tomonaga M, Kawasaki H, et al. Apolipoprotein E immunoreactivity in cerebral amyloid deposits and neurofibrillary tangles in Alzheimer's disease and kuru plaque amyloid in Creutzfeldt-Jakob disease. Brain Res 1991;541:163–66
53. Sagare A, Deane R, Bell RD, et al. Clearance of amyloid-beta by circulating lipoprotein receptors. Nat Med 2007;13:1029–31
54. Ito S, Ohtsuki S, Kamiie J, et al. Cerebral clearance of human amyloid-beta peptide (1–40) across the blood-brain barrier is reduced by self-aggregation and formation of low-density lipoprotein receptorrelated protein–1 ligand complexes. J Neurochem 2007;103: 2482–90
55. Quinn KA, Grimsley PG, Dai YP, et al. Soluble low density lipoprotein receptor–related protein (LRP) circulates in human plasma. J Biol Chem 1997;272:23946–51
56. Huang Y, Liu XQ, Wyss-Coray T, et al. Apolipoprotein E fragments present in Alzheimer's disease brains induce neurofibrillary tangle–like intracellular inclusions in neurons. Proc Natl Acad Sci U S A 2001;98: 8838–43
57. Bales KR, Verina T, Dodel RC, et al. Lack of apolipoprotein E dramatically reduces amyloid beta-peptide deposition. Nat Genet 1997; 17:263–64
58. Gallardo G, Schluter OM, Sudhof TC. A molecular pathway of neurodegeneration linking alpha-synuclein to ApoE and Abeta peptides. Nat Neurosci 2008;11:301–8
59. Greenow K, Pearce NJ, Ramji DP. The key role of apolipoprotein E in atherosclerosis. J Mol Med 2005;83:329–42
60. Yip AG, McKee AC, Green RC, et al. APOE, vascular pathology, and the AD brain. Neurology 2005;65:259–65
61. Ishigami M, Swertfeger DK, Hui MS, et al. Apolipoprotein E inhibition of vascular smooth muscle cell proliferation but not the inhibition of migration is mediated through activation of inducible nitric oxide synthase. Arterioscler Thromb Vasc Biol 2000;20:1020–26
62. Zhu Y, Hui DY. Apolipoprotein E binding to low density lipoprotein receptor–related protein–1 inhibits cell migration via activation of cAMP-dependent protein kinase A. J Biol Chem 2003;278:36257–63
63. Alafuzoff I, Adolfsson R, Grundke-Iqbal I, Winblad B. Blood-brain barrier in Alzheimer dementia and in non-demented elderly. An immunocytochemical study. Acta Neuropathol 1987;73:160–66
64. Alafuzoff I, Adolfsson R, Grundke-Iqbal I, Winblad B. Perivascular deposits of serum proteins in cerebral cortex in vascular dementia. Acta Neuropathol 1985;66:292–98
65. Ishii T, Haga S, Shimizu F. Identification of components of immunoglobulins in senile plaques by means of fluorescent antibody technique. Acta Neuropathol 1975;32:157–62
66. Zipser BD, Johanson CE, Gonzalez L, et al. Microvascular injury and blood-brain barrier leakage in Alzheimer's disease. Neurobiol Aging 2007;28:977–86
67. Clifford PM, Zarrabi S, Siu G, et al. Abeta peptides can enter the brain through a defective blood-brain barrier and bind selectively to neurons. Brain Res 2007;1142:223–36
68. Namba Y, Tsuchiya H, Ikeda K. Apolipoprotein B immunoreactivity in senile plaque and vascular amyloids and neurofibrillary tangles in the brains of patients with Alzheimer's disease. Neurosci Lett 1992;134: 264–66
69. Gentile MT, Poulet R, Pardo AD, et al. beta-Amyloid deposition in brain is enhanced in mouse models of arterial hypertension. Neurobiol Aging 2007 [Epub ahead of print]
70. Zhang SH, Reddick RL, Piedrahita JA, Maeda N. Spontaneous hypercholesterolemia and arterial lesions in mice lacking apolipoprotein E. Science 1992;258:468–71
71. Donahue JE, Johanson CE. Apolipoprotein E, amyloid-beta, and blood-brain barrier permeability in Alzheimer disease. J Neuropathol Exp Neurol 2008;67:261–70
72. Fullerton SM, Shirman GA, Strittmatter WJ, Matthew WD. Impairment of the blood-nerve and blood-brain barriers in apolipoprotein e knockout mice. Exp Neurol 2001;169:13–22
73. Morris JC. The Clinical Dementia Rating (CDR): Current version and scoring rules. Neurology 1993;43:2412–14

